

CSPMNet: Pareto-Efficient Automatic Modulation Classification With Learnable Complex Subband Phase Motion

Ruixiang Zhang, Zinan Zhou, Yezhuo Zhang, Guangyu Li and Xuanpeng Li

Abstract—Automatic modulation classification (AMC) is an essential technique for noncooperative spectrum monitoring and intelligent wireless receivers. However, practical AMC models must identify modulation formats from short and noisy I/Q observations while maintaining low computational and storage overhead. Existing deep-learning approaches often improve recognition accuracy by expanding generic neural backbones, which increases deployment cost and weakens their suitability for resource-constrained receivers. To bridge the gap between recognition performance and model efficiency, this letter proposes a Complex Subband Phase-Motion Network, designated as CSPMNet, for lightweight AMC from raw I/Q samples. Specifically, learnable complex subband filters are introduced to adaptively extract frequency-selective baseband responses while preserving the algebraic coupling between in-phase and quadrature components. Then, an amplitude-preserving phase-motion module captures multi-lag temporal rotation dynamics within each subband, and a lightweight temporal classifier performs efficient sequence aggregation. Rigorous experimental evaluations on public RadioML benchmark datasets demonstrate that CSPMNet achieves highly competitive recognition accuracy while requiring substantially lower model complexity than many existing AMC models. Codes are available on GitHub.

Index Terms—Automatic modulation classification, complex convolution, cognitive radio, lightweight neural networks.

I. INTRODUCTION

AUTOMATIC modulation classification (AMC) enables a noncooperative receiver to infer the modulation format of an observed I/Q sequence without transmitter-side metadata [1]. This function is required in cognitive radio, spectrum monitoring, and interference analysis, where unknown signals must be identified before demodulation or protocol-level processing. In practical sensing receivers, the observation is often short and noisy, and the classifier must remain small enough for repeated spectrum sensing. Although recent deep AMC models [2] enhance recognition by expanding network

capacity to learn from raw I/Q sequences or statistical features, sustaining satisfactory classification robustness within a stringent computational budget remains a critical bottleneck.

This difficulty primarily stems from the representation burden placed on compact classifiers [3], [4]. To reliably distinguish diverse modulation formats, an AMC model must simultaneously capture distinct spectral characteristics, amplitude variations, and phase dynamics from short baseband I/Q sequences [5], [6]. While scaling up network capacity helps learn these coupled physical factors, it often leads to high-complexity or even multi-million-parameter backbones that are ill-suited for edge sensing [3]. Conversely, merely shrinking the network size to lower computational costs often expels crucial modulation-discriminative details [4]. Therefore, to break this Pareto dilemma, an efficient AMC model should shift the representation burden to a physics-guided front-end, which explicitly injects complex-valued algebraic constraints and stabilizes noise-sensitive physical domains before decision-making.

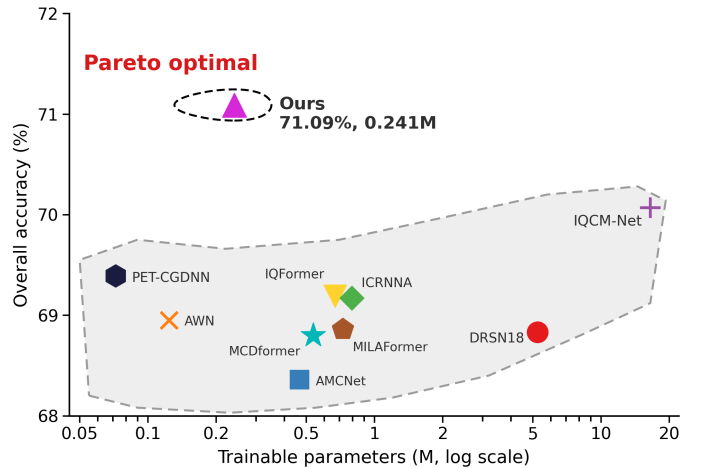


Fig. 1. Accuracy-parameter tradeoff on RadioML2022.01A.

To implement such a physics-guided front-end, this letter introduces CSPMNet, a learnable Complex Subband Phase-Motion Network designed for Pareto-efficient AMC. As quantified by the accuracy-parameter frontier visualized in Fig. 1, CSPMNet improves the accuracy-parameter tradeoff. Specifically, under a rigorous benchmark protocol on RadioML2022.01A [7], CSPMNet achieves an overall accuracy of 71.09% with a mere 0.241M trainable parameters, creating

arXiv:2605.25099v1 [eess.SP] 24 May 2026

This work has been submitted to the IEEE for possible publication. Copyright may be transferred without notice, after which this version may no longer be accessible. *Corresponding author: Xuanpeng Li*

Ruixiang Zhang, Zinan Zhou, Yezhuo Zhang and Xuanpeng Li are with the School of Instrument Science and Engineering, Southeast University, Nanjing, 210096, Jiangsu, China (e-mail: zhang_ruixiang@seu.edu.cn; zhouzinan919@seu.edu.cn; zhang_yezhuo@seu.edu.cn; li_xuanpeng@seu.edu.cn).

Guangyu Li is with the School of Computer Science and Engineering, University of Science and Technology, Nanjing, 210094, Jiangsu, China (email: guangyu.li2017@njust.edu.cn).

Digital Object Identifier XX.XXXX/LWC.2024.XXXXXXXX

a distinctly favorable Pareto operating point that outperforms both parameter-heavy and existing lightweight networks. By incorporating the inherent physical priors into the network front-end, CSPMNet reduces the representation pressure on subsequent neural layers. The main contributions of this letter are as follows:

- We introduce learnable complex subband into AMC from raw I/Q samples. This design replaces fixed transform preprocessing with task-adaptive complex filtering, preserving I/Q coupling and exposing frequency-selective signal components before lightweight recognition.
- We delve into amplitude-aware phase-motion modeling on the learned subbands. By constructing multi-lag complex phase-motion products together with magnitude reliability, the proposed representation avoids relying on phase-only angular cues and retains temporal rotation information that magnitude-only summaries may discard.
- Our CSPMNet demonstrates strong Pareto-efficient performance. Compared with reproduced benchmark models, it delivers higher recognition accuracy with substantially fewer trainable parameters, and maintains robust performance across low-, mid-, and high-SNR regimes.

II. PROBLEM DESCRIPTION

For a modulated signal with modulation type m , the received continuous-time waveform is modeled as

$$r(t) = \psi_m(s(t)) * p(t) + n(t), \quad (1)$$

where $s(t)$ denotes the transmitted symbol, $\psi_m(\cdot)$ is the modulation mapping associated with class m , $p(t)$ is the channel impulse response, $n(t)$ is additive white Gaussian noise, and $*$ denotes convolution. After down-conversion and sampling, each received sample is represented by an I/Q sequence

$$x = \begin{bmatrix} I[0], I[1], \dots, I[T-1] \\ Q[0], Q[1], \dots, Q[T-1] \end{bmatrix} \in \mathbb{R}^{2 \times T}, \quad (2)$$

where $I[\cdot]$ and $Q[\cdot]$ are the in-phase and quadrature-phase components. In the benchmarks used in this letter, $T = 128$.

Let $\mathcal{D} = \{(x_i, y_i)\}_{i=1}^N$ denotes a labeled AMC dataset, where y_i belongs to the candidate modulation set $\mathcal{C} = \{c_1, c_2, \dots, c_C\}$. AMC aims to learn a classifier $h_\theta: \mathbb{R}^{2 \times T} \rightarrow \mathbb{R}^C$, where $h_\theta(x)_c$ denotes the predicted score for modulation class c . The predicted label is then obtained by

$$\hat{y} = \arg \max_{c \in \mathcal{C}} h_\theta(x)_c. \quad (3)$$

This letter considers lightweight AMC, where the expected classification loss should be minimized under a limited model budget:

$$\min_{\theta} \mathbb{E}_{(x,y)}[\ell(h_\theta(x), y)], \quad \text{s.t.} \quad P(\theta) \leq B, \quad (4)$$

where $\ell(\cdot)$ is the classification loss, $P(\theta)$ denotes the number of trainable parameters, and B is the parameter budget. Under a small B , the classifier has limited capacity to learn rich modulation-discriminative features, motivating an explicit front-end for lightweight classification.

III. PROPOSED METHOD

A. Overall Architecture of CSPMNet

To reduce the representation burden, CSPMNet first transforms the raw I/Q sequence into a signal-informed feature map and then performs lightweight temporal aggregation. As shown in Fig. 2, the framework contains three consecutive components: a learnable complex subband front end, an amplitude-preserving subband phase-motion module, and a lightweight temporal classifier. The central design principle is to expose modulation-relevant complex dynamics before the final classifier, rather than relying on a large generic backbone to learn feature implicitly.

Given the input $x \in \mathbb{R}^{2 \times T}$, the first component generates a bank of complex subband responses by trainable complex filtering. The second component computes base response features and multi-lag phase-motion products within each subband while preserving amplitude reliability. The resulting sequence is finally fed into a lightweight classifier for modulation prediction. Unlike fixed-transform preprocessing followed by a heavy classifier, these components are trained jointly for the AMC objective, which allows the front end to adapt to modulation-discriminative subbands while keeping the downstream classifier modest.

B. Learnable Complex Subband Front End

The first component aims to separate frequency-selective signal structures without discarding the algebraic relation between the in-phase and quadrature components. Instead of treating the two input channels as unrelated real-valued features, CSPMNet applies S trainable complex filters to the baseband sequence. For subband s , the real and imaginary responses are

$$y_{s,r} = x_r * w_{s,r} - x_i * w_{s,i}, \quad y_{s,i} = x_r * w_{s,i} + x_i * w_{s,r}, \quad (5)$$

where x_r and x_i denote the in-phase and quadrature components of the input sequence, $*$ denotes one-dimensional convolution, and $w_{s,r}$ and $w_{s,i}$ are the real and imaginary components of the s -th complex filter, respectively. This operation follows the multiplication rule of complex convolution, so the real and imaginary parts are mixed as a coupled complex response rather than as two independent feature streams. Such a constraint is useful for AMC because modulation differences are often expressed through joint amplitude-phase behavior in the I/Q plane. The learned subband response is written as

$$z_s[n] = y_{s,r}[n] + jy_{s,i}[n] \quad (6)$$

and serves as a complex subband envelope for subsequent phase-motion extraction.

Compared with fixed wavelet or scattering filters, the free complex filters can adapt their passbands to the target AMC objective. Compared with unconstrained real-valued feature extraction, however, the front end still retains a signal-processing form: each filter produces a complex subband signal, and all subsequent phase-motion terms are computed from this response. This design therefore combines task adaptivity with an interpretation close to the original baseband representation.

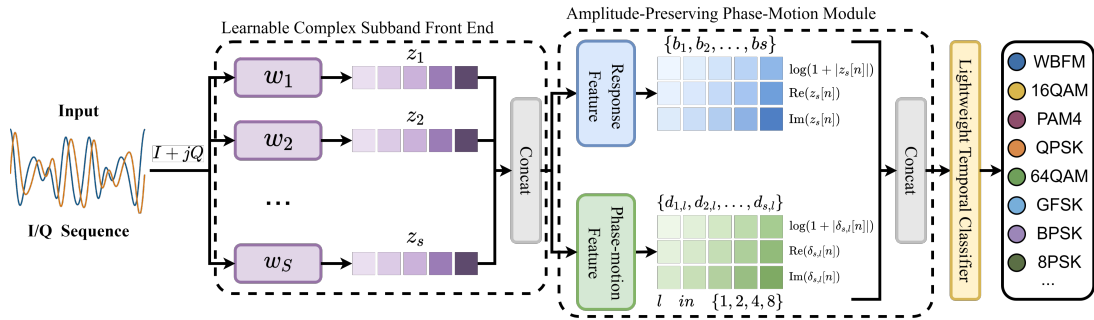


Fig. 2. Architecture of CSPMNet.

C. Amplitude-Preserving Phase-Motion Module

After subband filtering, the second component describes how the complex response evolves over time. AMC requires both amplitude and phase dynamics. Amplitude evolution is discriminative in itself, since envelope and subband-energy patterns help separate constant-envelope modulations from amplitude-varying ones and reflect constellation-level changes. Meanwhile, phase increments and rotations characterize temporal angular motion, but their reliability depends on local signal energy under noise. This is particularly important under low-SNR conditions. If a phase descriptor is normalized to a unit-magnitude angular feature, a weak noise-dominated response may be assigned the same strength as a high-energy signal component. Conversely, a magnitude-only descriptor may suppress the direction and rotation information that separates modulation families. Therefore, CSPMNet constructs subband phase-motion features without removing amplitude reliability.

For each subband response $z_s[n]$, the response features are

$$b_s[n] = [\log(1 + |z_s[n]|), \text{Re}(z_s[n]), \text{Im}(z_s[n])]. \quad (7)$$

For each lag l in $\{1, 2, 4, 8\}$, the complex phase-motion product is

$$\delta_{s,l}[n] = z_s[n] \text{conj}(z_s[n-l]), \quad (8)$$

from which the model extracts

$$d_{s,l}[n] = [\log(1 + |\delta_{s,l}[n]|), \text{Re}(\delta_{s,l}[n]), \text{Im}(\delta_{s,l}[n])]. \quad (9)$$

The product $\delta_{s,l}[n]$ measures the complex rotation between two samples separated by lag l . The lag set $\{1, 2, 4, 8\}$ covers both short-range and longer-range temporal dynamics within each subband. By concatenating $b_s[n]$ and all $d_{s,l}[n]$ across the eight subbands, CSPMNet obtains a feature map at each time index. The classifier therefore receives not only the direction of subband phase motion, but also the magnitude of the underlying response and of the phase-motion product. This amplitude-preserving formulation distinguishes the proposed representation from phase-only angular descriptors and prevents unreliable low-energy phase estimates from being treated as equally confident evidence.

D. Lightweight Temporal Classifier

The final component aggregates the subband phase-motion sequence into a modulation prediction. Because the preceding

 TABLE I
 DETAILED PARAMETERS OF DATASETS

Parameter	RadioML2022.01A	RadioML2016.10B
Modulation number	11	10
Signal length	128	128
SNR range	-20:2:20 dB	-20:2:18 dB
Samples per mod.	42,000	20,000

modules already expose frequency-selective and amplitude-aware phase dynamics, the classifier is designed to remain compact rather than to act as a large feature extractor. The feature map is first normalized by `BatchNorm1d` and mixed by a one-dimensional convolution. A one-layer bidirectional GRU then models temporal dependencies in the phase-motion sequence, and scaled additive attention pools the sequence by assigning larger weights to more discriminative time positions. The representation is finally passed to a small MLP classifier.

This lightweight head matches the overall goal of Pareto-efficient AMC. The convolution performs local channel mixing, the bidirectional GRU captures short temporal context, and the attention layer replaces uniform averaging with data-dependent temporal pooling. Together with the small subband front end, the full CSPMNet contains 240,972 trainable parameters. Thus, the proposed model concentrates capacity on modulation-oriented representation construction while remaining much smaller than large backbones.

IV. EXPERIMENTAL RESULTS AND ANALYSIS

A. Implementation Details

The main evaluation is conducted on RadioML2022.01A [7], and the secondary evaluation is conducted on RadioML2016.10B [8]. The detailed dataset parameters are listed in Table I. RadioML2022.01A contains 11 modulation classes and 21 SNR points, while RadioML2016.10B contains 10 modulation classes and 20 SNR points.

All models are implemented in Python 3.10 with PyTorch 2.4.1 and CUDA 12.4, and trained on NVIDIA GeForce RTX 3080 GPUs using the Adam optimizer. Unless otherwise stated, all results use a fixed per-modulation per-SNR split with an effective train/validation/test ratio of 60/20/20, seed 42, 50 training epochs, batch size 512, and learning rate 1×10^{-3} . Baselines are reproduced under the same split protocol, including DRSN18[9], ICRNNA[10], IQFormer[11], AMCNet[6], AWN[4], IQCM-Net[2], MCDformer[5],

TABLE II
PERFORMANCE AND COMPLEXITY COMPARISON ON BENCHMARK DATASETS

Model	Complexity		Performance Metrics (%)			
	Params (M)	FLOPs (M)	OA	Low SNR	Mid SNR	High SNR
				≤ -10 dB	$-8-0$ dB	≥ 2 dB
RadioML2022.01A						
PET-CGDNN	0.072	16.24	69.39	26.30	69.40	95.24
AWN	0.124	11.97	68.95	26.24	68.00	95.04
IQFormer	0.670	89.07	69.19	25.58	68.58	95.67
ICRNNA	0.795	10.78	69.17	25.95	68.93	95.23
MCDformer	0.537	198.80	68.80	26.46	68.82	94.20
MILAFormer	0.726	80.50	68.86	26.58	68.38	94.47
AMCNet	0.466	92.64	68.36	25.11	68.19	94.40
DRSN18	5.250	176.96	68.83	26.34	68.41	94.54
IQCM-Net	16.482	848.39	<u>70.07</u>	<u>26.93</u>	<u>70.53</u>	<u>95.73</u>
CSPMNet (Ours)	0.241	49.98	71.09	28.25	71.94	96.37
RadioML2016.10B						
PET-CGDNN	0.072	16.24	60.84	16.42	62.66	89.44
AWN	0.124	11.97	61.97	15.59	66.19	90.53
IQFormer	0.670	89.07	62.48	17.20	63.97	91.83
ICRNNA	0.795	10.78	60.24	14.39	63.26	89.13
MCDformer	0.537	198.80	62.37	15.08	<u>67.89</u>	90.83
MILAFormer	0.726	80.50	63.15	<u>16.91</u>	66.65	92.03
AMCNet	0.466	92.64	57.88	14.96	58.93	85.91
DRSN18	5.250	176.96	61.18	14.82	64.61	90.17
IQCM-Net	16.482	848.39	<u>63.19</u>	16.67	65.94	92.67
CSPMNet (Ours)	0.241	49.98	63.26	15.18	68.35	<u>92.49</u>

FLOPs are estimated using PyTorch FlopCounterMode under input shape $1 \times 2 \times 128$; all models are profiled with the same script and environment.

MILAFormer[12] and PET-CGDNN[3]. Trainable parameter counts are computed from the local model implementations.

B. Experiment Results

1) *Accuracy-Complexity Comparison*: Table II compares CSPMNet with baselines in terms of trainable parameters, FLOPs, overall accuracy (OA) and SNR-segment accuracy.

On RadioML2022.01A, CSPMNet achieves the best OA of 71.09% and also ranks first in the low-, mid-, and high-SNR averages. Compared with IQCM-Net, the strongest reproduced baseline in OA, CSPMNet improves OA by 1.02 percentage points while reducing the parameter count from 16.482M to 0.241M and FLOPs from 848.39M to 49.98M. This corresponds to about $68.4\times$ fewer parameters and $17.0\times$ fewer FLOPs. Compared with the lightweight AWN baseline, CSPMNet improves OA by 2.14 percentage points and increases the low-, mid-, and high-SNR averages by 2.01, 3.94, and 1.33 percentage points, respectively, while still keeping the model below 0.25M parameters and 50M FLOPs.

CSPMNet is not the model with the absolute minimum computational cost. ICRNNA, AWN and PET-CGDNN have lower FLOPs or fewer parameters. However, their OA values on RadioML2022.01A remain below 69.40%, and their low-, mid-, and high-SNR averages are all lower than those of CSPMNet. Thus, the proposed model does not simply trade accuracy for compactness; rather, it uses a moderate computational budget to move beyond existing lightweight baselines while avoiding the cost of a large cross-modal backbone.

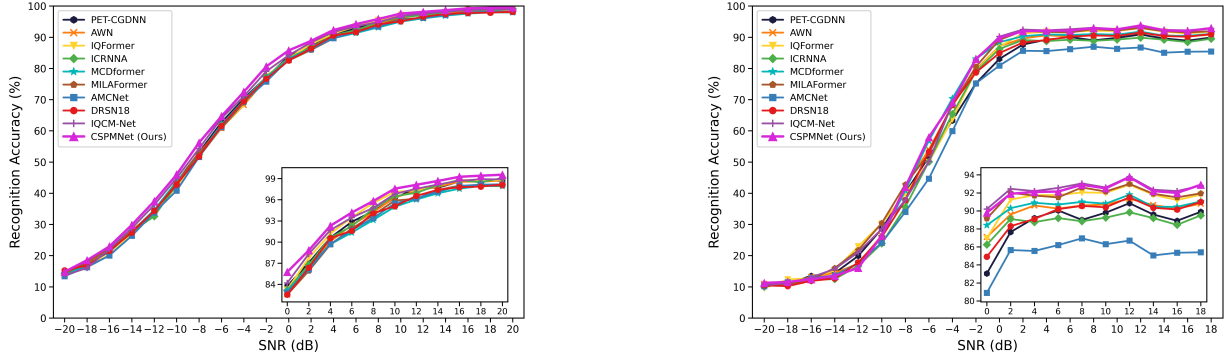
On RadioML2016.10B, CSPMNet achieves comparable overall accuracy to the strongest reproduced baselines while

using substantially fewer parameters. Compared with IQCM-Net, it gives a small OA gain of about 0.08 percentage points while retaining the same $68.4\times$ parameter reduction and $17.0\times$ FLOP reduction. Its high-SNR average remains close to IQCM-Net, whereas its low-SNR average is not the best. Overall, the RadioML2016.10B results support the efficiency and competitiveness of CSPMNet, rather than implying uniform dominance across all SNR regimes.

2) *SNR-Wise Analysis*: To further evaluate robustness under different channel qualities, Fig. 3 compares the recognition accuracy of CSPMNet and other AMC models at each SNR point. As shown in Fig. 3(a), CSPMNet achieves the best accuracy at 20 of the 21 SNR points on RadioML2022.01A. The only exception is -20 dB, where it is slightly lower than DRSN18 by 0.45 percentage points. Compared with IQCM-Net, CSPMNet maintains positive gains at all SNR points, with the largest gain of 2.48 percentage points appearing at -18 dB. Compared with the lightweight AWN baseline, the largest gain appears at -8 dB and reaches 4.50 percentage points.

The advantage is most evident from the low-to-transition region to 0 dB. In this interval, noise is still strong enough to disturb modulation cues, but the signal is no longer completely unrecoverable. This trend is consistent with the motivation of amplitude-preserving phase-motion modeling, where temporal phase dynamics become informative while magnitude reliability helps suppress weak noise-dominated responses. As a result, CSPMNet achieves the best low-, mid-, and high-SNR averages on RadioML2022.01A, as reported in Table II.

Fig. 3(b) shows a more bounded trend on RadioML2016.10B. CSPMNet does not dominate most



(a) RadioML2022.01A

(b) RadioML2016.10B

Fig. 3. Recognition accuracy of CSPMNet and other AMC models under different SNRs. (a) RadioML2022.01A. (b) RadioML2016.10B.

TABLE III

ABLATION STUDY ON RADIOML2022.01A AND RADIOML2016.10B

Variant	RadioML2022.01A	RadioML2016.10B
PhaseMotion only	61.36 (↓ 9.73)	59.30 (↓ 3.96)
Fixed Morlet subband	57.51 (↓ 13.58)	56.45 (↓ 6.81)
Learnable Morlet subband	69.01 (↓ 2.08)	57.68 (↓ 5.58)
CSPMNet	71.09	63.26

individual SNR points, but it tracks the strongest curves from the transition region upward and achieves the best average accuracy over $-8-0$ dB. In this mid-SNR interval, it exceeds IQCM-Net by 2.41 percentage points and MCDformer by 0.46 percentage points. At high SNRs, CSPMNet remains close to IQCM-Net, while its low-SNR average is not the best. Thus, the per-SNR curves support the same interpretation as Table II: CSPMNet is strongest on RadioML2022.01A and remains competitive on RadioML2016.10B without implying uniform pointwise dominance.

3) *Ablation Study*: To evaluate the contribution of the model design, we compare CSPMNet with three variants on both datasets. As shown in Table III, all variants are less accurate than CSPMNet on both datasets. Using phase-motion features without learnable subband filtering, or replacing the free complex subband filters with fixed or constrained Morlet filters, consistently reduces OA. This indicates that the proposed modules play a positive role in CSPMNet.

V. CONCLUSION

In this letter, we propose CSPMNet, a Complex Subband Phase-Motion Network for efficient AMC from raw I/Q samples. The proposed model enhances the accuracy-complexity tradeoff by incorporating learnable complex subband filtering and amplitude-preserving phase-motion modeling into a lightweight temporal classifier. Experimental results on benchmark datasets demonstrate that CSPMNet, compared with existing AMC models, not only achieves highly competitive recognition performance but also benefits from substantially reduced model complexity, making it suitable for lightweight spectrum-monitoring receivers. Moreover, the proposed front end improves the extraction of modulation-discriminative subband dynamics across different SNR conditions. These results indicate that physics-guided complex front ends have

practical potential for efficient AMC in resource-constrained communication scenarios. Future work will explore adaptive complex subband modeling within AMC to further extend physics-guided representation learning toward more dynamic and heterogeneous spectrum environments.

REFERENCES

- [1] S. Peng, S. Sun, and Y.-D. Yao, "A survey of modulation classification using deep learning: Signal representation and data preprocessing," *IEEE Transactions on Neural Networks and Learning Systems*, vol. 33, no. 12, pp. 7020–7038, 2021.
- [2] J. Li, M. Huang, J. Yang, and Z. Xiao, "Iqcm-net: Cross-modal fusion with multi-window stft via snr partitioning for robust modulation recognition," *IEEE Transactions on Cognitive Communications and Networking*, 2026.
- [3] F. Zhang, C. Luo, J. Xu, and Y. Luo, "An efficient deep learning model for automatic modulation recognition based on parameter estimation and transformation," *IEEE Communications Letters*, vol. 25, no. 10, pp. 3287–3290, 2021.
- [4] J. Zhang, T. Wang, Z. Feng, and S. Yang, "Toward the automatic modulation classification with adaptive wavelet network," *IEEE Transactions on Cognitive Communications and Networking*, vol. 9, no. 3, pp. 549–563, 2023.
- [5] Z. Chen, X. Zhang, and K. He, "Multi-channel convolutional distilled transformer for automatic modulation classification," in *2024 International Joint Conference on Neural Networks (IJCNN)*. IEEE, 2024, pp. 1–8.
- [6] J. Zhang, T. Wang, Z. Feng, and S. Yang, "Amc-net: An effective network for automatic modulation classification," in *ICASSP 2023-2023 IEEE International Conference on Acoustics, Speech and Signal Processing (ICASSP)*. IEEE, 2023, pp. 1–5.
- [7] V. Sathyanarayanan, P. Gerstoft, and A. El Gamal, "Rml22: Realistic dataset generation for wireless modulation classification," *IEEE Transactions on Wireless Communications*, vol. 22, no. 11, pp. 7663–7675, 2023.
- [8] T. J. O'shea and N. West, "Radio machine learning dataset generation with gnu radio," in *Proceedings of the GNU radio conference*, vol. 1, no. 1, 2016.
- [9] M. Zhao, S. Zhong, X. Fu, B. Tang, and M. Pecht, "Deep residual shrinkage networks for fault diagnosis," *IEEE Transactions on Industrial Informatics*, vol. 16, no. 7, pp. 4681–4690, 2019.
- [10] N. El-Haryqy, A. Kharbouche, H. Ouamna, Z. Madini, and Y. Zouine, "Improved automatic modulation recognition using deep learning with additive attention," *Results in Engineering*, vol. 26, p. 104783, 2025.
- [11] M. Shao, D. Li, S. Hong, J. Qi, and H. Sun, "Iqformer: A novel transformer-based model with multi-modality fusion for automatic modulation recognition," *IEEE Transactions on Cognitive Communications and Networking*, vol. 11, no. 3, pp. 1623–1634, 2024.
- [12] J. Zhao, Y. Sun, Y. Chen, X. Dong, G. Song, N. Jin, and D. Quan, "Milaformer: A multi-stage hybrid deep learning architecture for robust radio signal modulation recognition," *IEEE Transactions on Cognitive Communications and Networking*, 2026.